



**HAL**  
open science

## Vertical variations in wood basic density for two softwood species

Antoine Billard, Rodolphe Bauer, Mothe Frédéric, Francis Colin, Christine Deleuze, Fleur Longuetaud

### ► To cite this version:

Antoine Billard, Rodolphe Bauer, Mothe Frédéric, Francis Colin, Christine Deleuze, et al.. Vertical variations in wood basic density for two softwood species. *European Journal of Forest Research*, 2021, 140, pp.1401-1416. 10.1007/s10342-021-01402-y . hal-03334029

**HAL Id: hal-03334029**

**<https://hal.science/hal-03334029v1>**

Submitted on 29 Aug 2024

**HAL** is a multi-disciplinary open access archive for the deposit and dissemination of scientific research documents, whether they are published or not. The documents may come from teaching and research institutions in France or abroad, or from public or private research centers.

L'archive ouverte pluridisciplinaire **HAL**, est destinée au dépôt et à la diffusion de documents scientifiques de niveau recherche, publiés ou non, émanant des établissements d'enseignement et de recherche français ou étrangers, des laboratoires publics ou privés.

# Vertical variations in wood basic density for two softwood species

Antoine Billard<sup>a,b,\*</sup>, Rodolphe Bauer<sup>a</sup>, Frédéric Mothe<sup>a</sup>, Francis Colin<sup>a</sup>, Deleuze Christine<sup>c</sup>,  
Fleur Longuetaud<sup>a</sup>

<sup>a</sup>Université de Lorraine, AgroParisTech, INRAE, Silva, 54000 Nancy, France

<sup>b</sup>Agence de la transition écologique, 20 Avenue du Grésillé, BP 90406, 49004 Angers Cedex 01, France

<sup>c</sup>RDI, ONF, 39100 Dole, France

---

## Abstract

Studies on wood basic density ( $BD$ ) vertical variations become essential to predict more accurately the within-stem distributions of biomass and wood quality in the forest resource. The vertical variation of wood  $BD$  in the stem has been little studied until now, most  $BD$  studies being based on measurements taken at breast height.

The main objective of this work was to observe and to understand the patterns of vertical  $BD$  variation within stems in relation to classical dendrometric variables and to propose relevant equation forms for future modelling.

Two softwood species were studied: *Abies alba* and *Pseudotsuga menziesii*. Contrasted thinning intensities were studied including strongly thinned plots *versus* control plots without thinning.

$BD$  was most of the time highest at the base of the tree for both species. Then, after a strong decrease from the base of the tree, an increase in  $BD$  was often observed towards the top of the tree especially for *Abies alba*.

The variation in  $BD$  with height was stronger for the unthinned plots than for the heavily thinned ones of *Abies alba*. The opposite was observed for *Pseudotsuga menziesii*. The modulation of growth rate and tree size through thinning intensities modifies the observed vertical variations in  $BD$ .

Two types of biexponential models were proposed to describe  $BD$  variations. The first

---

\*Corresponding author

Email addresses: antoine.billard@inrae.fr (Antoine Billard), rodolphe.bauer@inrae.fr (Rodolphe Bauer), frederic.mothe@inrae.fr (Frédéric Mothe), francis.colin@inrae.fr (Francis Colin), christine.deleuze@onf.fr (Deleuze Christine), fleur.longuetaud@inrae.fr (Fleur Longuetaud)

model used the height in the stem and classical easily-measurable tree variables as inputs, the other one additionally used  $BD$  at breast height ( $BD130$ ).

The relative RMSE of  $BD$  for *Abies alba* and *Pseudotsuga menziesii* were 9.9% and 8.1%, respectively, with the model without  $BD130$  and 7.6% and 5.9%, respectively, with the model including  $BD130$ .

*Keywords:* Basic specific gravity, axial variations, thinning intensity, *silver fir*, *Douglas fir*

---

## 1. Introduction

The modalities of wood formation and the variability of wood properties are being gradually discovered. Wood performs several functions that enable the development of the tree itself and the structuring of forest ecosystems. It provides numerous ecological services such as carbon fixation and economic services through its various uses accompanying human activities (timber, industrial wood, wood for energy, wood for chemical purposes).

Among the characteristics of wood, density is a critical property that is linked on the one hand with the composition and anatomy of its constituent tissues and on the other hand with other wood properties such as strength, stiffness and pulp yield (Barnett and Jeronimidis, 2003). Density is basically a measure of the mass of material in a given volume (Zobel and Van Buijtenen, 1989). Basic density ( $BD$ ) is defined by the ratio of the oven-dried mass of wood to the corresponding volume of green (or fresh) wood. The volume of green wood is a variable commonly measured and used by foresters and for forest inventories. Many models exist to predict the green aboveground woody volume of trees for most temperate tree species (Henry et al., 2013), whether it is the total aboveground volume or the stem volume, total or up to a given stem diameter. The oven-dried mass of a wood sample can be obtained after drying at 103°C in an oven (Williamson and Wiemann, 2010). The knowledge of the mean  $BD$  of tree (or stem) makes it possible to convert the green volume of tree (or stem) to dry mass of matter. Then, the product of dry mass by carbon fraction allows to account for stored carbon (Wiemann and Williamson, 2014; Bouriaud et al., 2015). Similar calculations can be used to estimate the quantities of various extractive compounds available in the resource.

Wood density is highly variable at all levels. It varies between species, between trees of a

24 given species and within trees. Many studies have already focused on the evaluation of wood  
25  $BD$  of most species. They led to the creation of global databases, such as the Global Wood  
26 Density Database (Zanne et al., 2009), which provides mean  $BD$  for many species around  
27 the world. However, such databases derived from literature data should be used with caution  
28 and it is advised to check which density was measured, how it was measured and which is  
29 the area of validity of each study (Taras and Wahlgren, 1963; Williamson and Wiemann,  
30 2010). For instance, some studies provide air-dried density (i.e., the ratio of air-dried mass  
31 to air-dried volume) that needs to be converted to  $BD$ . Conversion errors are possible as  
32 shown by Vieilledent et al. (2018) who have started to correct the Global Wood Density  
33 Database.

34 Most studies have analysed mean wood density at breast height only. Others have taken  
35 the knowledge a step further by looking at the radial variations in  $BD$  on cores or discs,  
36 taken most often at breast height only (Wahlgren and Fassnacht, 1959; Woodcock and Shier,  
37 2002; Deng et al., 2014).

38 A general result is that, for most softwoods, the ring density decreases when ring width  
39 increases. This is explained by the fact that the wider the rings, the greater the proportion of  
40 earlywood made up of thin-walled tracheids and wide lumens dedicated to hydraulic conduc-  
41 tion. At the same time the width of the latewood, more dedicated to mechanical resistance,  
42 remains relatively constant. Generally speaking, for these softwood species, it is expected  
43 that the more heavy the thinning, the wider the growth rings and the lower the density of  
44 the wood.

45 This is generally true for species showing a gradual transition between earlywood and  
46 latewood like *Abies* or *Picea* spp.. This is less clear for *Pseudotsuga menziesii*, for example,  
47 which shows an abrupt transition between earlywood and latewood (Todaro and Macchioni,  
48 2011). And finally the results about the relationship between ring width and wood density  
49 are often conflicting (Jozsa et al., 1994).

50 Juvenile wood is also often cited as a factor influencing wood density. Larson et al.  
51 (2001) gives the definition of juvenile wood as the wood formed in the first three years of a  
52 tree. Then, the formed wood near the pith will be corewood, regardless of the height in the  
53 tree. Corewood is often confused with juvenile wood. The properties of corewood are highly

54 variable, especially the wood density. According to Lachenbruch et al. (2011), for softwoods  
55 in the Pacific Northwest of North America,  $BD$  generally decreases approximately for ring  
56 numbers 5 to 20, then increases (sometimes only increases in particular for hard pines). The  
57 transition from corewood to outerwood (or mature wood) is usually soft. The corewood has  
58 a lower  $BD$  than mature wood (10–20% of differences). In this article, the term “juvenile  
59 wood” will be used for both juvenile wood and corewood.

60 Vertical (or axial) variations in density have been much less studied than radial variations.  
61 There is, however, a real influence of vertical variations on the mean density of the whole  
62 stem that can differ significantly from the density at breast height (Nogueira et al., 2008;  
63 Wiemann and Williamson, 2014; Wassenberg et al., 2015; Longuetaud et al., 2016, 2017).  
64 Studying the vertical variations of wood density allows to refine biomass estimates as well as  
65 carbon accounting (Rueda and Williamson, 1992; Liepiņš and Liepiņš, 2017). This knowledge  
66 is also required to assess accurately the amount and quality of the wood resource depending  
67 on the location along the stem (Tian et al., 1995; Kimberley et al., 2015). And this detailed  
68 description should make it possible to optimize the use of the resource for different purposes.  
69 Indeed, numerous wood properties are correlated to wood density, like mechanical properties  
70 (Niklas and Spatz, 2010), dimensional stability (Hernández, 2007) or durability (Humar et al.,  
71 2008) that are of peculiar importance for the structural uses of wood, especially for softwoods.  
72 Fuelwood properties can also be related to wood density (Sotelo Montes et al., 2017) as well  
73 as paper properties (García-Gonzalo et al., 2016). Moreover, the stem volume represents  
74 about 80% of the total aboveground woody volume for softwoods and the precision on such  
75 a large volume cannot be neglected (Billard et al., 2020).

76 Density variations with height can be related to radial variations due to cambial age,  
77 ring width or juvenile wood, especially for species showing strong radial variations in density.  
78 For instance, the mean wood density at a given height can be related to the proportion of  
79 juvenile wood at that height, especially for species showing a strong difference in density  
80 between juvenile wood and mature wood (Zobel and Van Buijtenen, 1989).

81 For softwoods, the density seems to decrease from the bottom of the tree to the top  
82 (Gartner et al., 2002; Longuetaud et al., 2017). Sometimes, a U-shaped curve was observed,  
83 especially for *Picea abies* which is the most widely studied species (Repola, 2006; Molteberg

84 and Høibø, 2007; Liepiņš and Liepiņš, 2017). The decrease in density between the bottom  
85 and the top of the stem was also observed for *Ps. menziesii* (Kimberley et al., 2017) and  
86 *Abies alba* (González-Rodrigo et al., 2013).

87 Some authors have proposed models for describing the vertical variations in density in the  
88 stem. Table 1 presents models which provides wood  $BD$  at different heights. Most models  
89 are linear models, often of polynomial form (among others, Rueda and Williamson, 1992;  
90 Tian et al., 1995; Repola, 2006; Molteberg and Høibø, 2007; González-Rodrigo et al., 2013;  
91 Deng et al., 2014). The main tree variables used in these models are tree total height ( $H$ )  
92 and diameter ( $D130$ ) or circumference at breast height ( $C130$ ). Sometimes the age of the  
93 tree was used.

94 Models using ring number or distance from the pith in addition to the height in the stem  
95 as input variable (e.g., Rueda and Williamson, 1992; Tian et al., 1995) are not presented here  
96 since this paper focuses on the mean  $BD$  of whole discs.

97 In this study, the vertical variations in  $BD$  of two softwood species were studied: *Abies*  
98 *alba* Mill. (*A. alba*) and *Pseudotsuga menziesii* (Mirb.) Franco (*Ps. menziesii*). These  
99 species are of major importance in the North-East of France and have the interest of being  
100 very different from an ecological point of view with contrasting shading tolerances (Niinemets  
101 and Valladares, 2006) and contrasted anatomical characteristics with more or less marked  
102 transitions between earlywood and latewood (Saranpää, 2003; Todaro and Macchioni, 2011).  
103 To our knowledge, there are almost no studies that address vertical variations in density for  
104 these species, except the one from Kimberley et al. (2017) on *Ps. menziesii* and the one from  
105 González-Rodrigo et al. (2013) on *A. alba*.

106 The main objective of this work was therefore to describe these vertical variations of  $BD$  in  
107 the stems and to propose some explanations for the observed patterns. For this purpose, new  
108 forms of models more easily extensible to new data than the previous polynomial approaches,  
109 have been proposed and fitted. Considering that  $BD$  at breast height can be relatively easily  
110 assessed by analysing core samples or by using dedicated models (Kerfriden et al., 2021), we  
111 have compared models using and not using this data as input. Such models may serve as a  
112 basis for future predictive modelling on a larger data set. To guide this work, and based on  
113 the literature, we have formulated four more specific hypotheses to which we will come back

114 with regard to our results in the discussion:

- 115 • **H1:** The proportion of juvenile wood in stem discs contributes to explain the  $BD$   
116 variations with height in the stem;
- 117 • **H2:** Stem discs showing the larger ring widths, regardless of their height in the tree,  
118 have a lower  $BD$  (i.e., the ring density-ring width well-known relationship for softwoods  
119 may be generalised to the average level of the whole disc, from different trees or different  
120 heights in the stem);
- 121 • **H3:** On the basis of **H1** and **H2**, the growth rate and/or tree size modulated by  
122 thinning intensities modifies the vertical variation of  $BD$  in the stems;
- 123 • **H4:**  $BD$  measured at breast height overestimates significantly the mean  $BD$  of the  
124 whole stem and as a consequence breast height measurements are not representative of  
125 the whole stem.

Table 1: Equations of the literature to model the mean basic density of a disc at a given height in the stem.  $BD_{disc}$  is the whole-disc mean density,  $BD130$  is the mean density at breast height,  $hr$  is the relative height of the disc,  $age$  is the age of the tree,  $D130$  is the diameter at breast height of the tree,  $H$  is the total tree height,  $b_0, \dots, b_5$  are the fixed-effect parameters,  $u_0, \dots, u_3$  are the random-effect parameters.

	Article	Species	Number of trees	Equation
Without $BD130$	Repola (2006)	<i>P. abies</i>	39	$BD_{disc} = b_0 + b_1 \cdot H + b_2 \cdot \frac{D130}{age} + b_3 \cdot hr$ $+ b_4 \cdot hr^2 + u_0 + u_1 \cdot hr + u_2 \cdot hr^2$
	González-Rodrigo et al. (2013)	<i>Abies alba</i>	5	$BD_{disc} = b_0 - b_1 \cdot H$
	Deng et al. (2014)	<i>Pinus massoniana</i>	108	$BD_{disc} = b_0 + b_1 \cdot age + b_2 \cdot D130 + b_3 \cdot hr + b_4 \cdot hr^2$ $+ b_5 \cdot hr^3 + u_0 + u_1 \cdot hr + u_2 \cdot hr^2 + u_3 \cdot hr^3$
With $BD130$	Kimberley et al. (2015)	<i>Pinus radiata</i>	10000	$h_k = \frac{1}{H} - 0.4$ $L_k = \frac{BD130 - b_0 - b_1 \cdot h_k - b_2 \cdot h_k^2 - b_3 \cdot h_k^3}{1 + b_4 \cdot h_k}$ $BD_{disc} = (b_0 + L_k) + (b_1 + b_4 \cdot L_k) \cdot (hr - 0.4)$ $+ b_2 \cdot (hr - 0.4)^2 + b_3 \cdot (hr - 0.4)^3$
	Kimberley et al. (2017)	<i>Ps. menziesii</i>	172	$h_k = \frac{1}{H}$ $L_k = BD130 - (b_0 + b_1 \cdot h_k + b_2 \cdot h_k^2 + b_3 \cdot h_k^3)$ $BD_{disc} = L_k + b_0 + b_1 \cdot hr + b_2 \cdot hr^2 + b_3 \cdot hr^3$ $= BD130 + b_1 \cdot (hr - h_k) + b_2 \cdot (hr^2 - h_k^2)$ $+ b_3 \cdot (hr^3 - h_k^3)$

Table 2: Table of abbreviations used in the article.

Abbreviation	Meaning
<i>BD</i>	Basic density ( $\text{kg} \cdot \text{m}^{-3}$ )
<i>BD130</i>	Basic density at breast height ( $\text{kg} \cdot \text{m}^{-3}$ )
<i>H</i>	Total height of the tree (m)
<i>h</i>	Height of the measure (m)
<i>hLLB</i>	Height of the lowest living branch (m)
<i>hLC</i>	Height to the base of the living crown (m)
<i>hr</i>	Relative height of the measure (%)
<i>hrLC</i>	Relative height of the living crown (%)
<i>D130</i>	Diameter at breast height (cm)
<i>C130</i>	Circumference at breast height (cm)
<i>RW130</i>	Mean ring width at breast height (mm)

## 126 2. Materials and Methods

127 All the abbreviations used in this paper are listed in Table 2.

### 128 2.1. Study sites and sampling design

129 The trees were sampled within the framework of two projects named “ExtraFor\_Est”  
130 and “ModelFor”. In both datasets, contrasted thinning intensities were tried out. For each  
131 species, trees from “ExtraFor\_Est” were selected from two plots: a plot without thinning  
132 (only natural mortality) and another one with heavy thinning. For each species, trees from  
133 “ModelFor” were selected from three plots: without thinning, moderate thinning and heavy  
134 thinning. Table 3 provides information about the stands. More information is available  
135 in Table A.1 of Appendix A. The trees came from the Office National des Forêts (ONF)  
136 experimental monitoring forest for which the history of the trees has been kept since the  
137 plantation. Moreover, *Ps. menziesii* from “ModelFor” came from the experimental network  
138 of Douglas stands managed by the *GIS Coop* (<https://www6.inrae.fr/giscoop>, Seynave  
139 et al. (2018))



140 Our forest identifiers have been constructed as follows: the first two letters correspond  
 141 to the species “Aa” means *Abies alba* and “Pm” means *Pseudotsuga menziesii*, the number  
 142 following these two letters 1, 2 or 3 represents the number of the forest (see Table 3 for more  
 143 details). These two letters and this number are sometimes followed by an hyphen and a  
 144 letter which represent the thinning modality. “-u” means unthinned modality, “-m” means  
 145 moderate thinning and “-h” means heavy thinning.

Table 3: Site characteristics.

Tree species	Forest	ID	Location	Altitude (m)	Number of trees	Age of trees	Project
<i>A. alba</i>	Saint-Prix	Aa1	46.97 N, 4.07 E	750	8	43-57	ExtraFor_Est
	Saint-Prix	Aa2	46.97 N, 4.07 E	750	14	36-80	ModelFor
	Mont-Sainte-Marie	Aa3	46.79 N, 6.31 E	1000	15	36-41	ModelFor
<i>Ps. menziesii</i>	Mélagues	Pm1	43.71 N, 3.06 E	800	8	48	ExtraFor_Est
	Grison	Pm2	46.66 N, 4.74 E	210	15	43	ModelFor
	Quartier	Pm3	46.15 N, 2.77 E	630	15	20	ModelFor

146 The trees from “ExtraFor\_Est” were cut in February 2018. The trees in each thinning  
 147 modality were classified into four diameter classes (defined by the 25<sup>th</sup>, 50<sup>th</sup> and 75<sup>th</sup> per-  
 148 centiles) and one tree was felled in each diameter class. The circumference at breast height  
 149 (1.30 m) was measured. After felling the trees, the total height and the height to the base  
 150 of the living crown (the lowest whorl with at least 3/4 of living branches) were measured.  
 151 A total of 15 discs were sampled along the stem, avoiding knots. The first three discs were  
 152 taken systematically at heights 0.3 m, 0.8 m and 1.30 m. The 12 other discs were regularly  
 153 distributed along the stem.

154 The same protocol was applied to the trees from “ModelFor” dataset except that the  
 155 number of discs depended on the tree length. Above breast height, the discs were sampled  
 156 every 2 m at the maximum. For *Ps. menziesii* of Grison and Quartier forests, five trees  
 157 per thinning modality were chosen in order to represent the different diameters present in  
 158 the plot (i.e., one tree in each of the five diameter classes based on the 20<sup>th</sup>, 40<sup>th</sup>, 60<sup>th</sup> and  
 159 80<sup>th</sup> percentiles), resulting in 15 trees per forest. For *A. alba*, 14 trees per forest were felled  
 160 (and one more at Mont-Sainte-Marie). There were four trees sampled in heavy thinning and  
 161 moderate thinning modalities (five in moderate thinning modality at Mont-Sainte-Marie) and  
 162 six trees in the plot without thinning. The number of trees per thinning modality is given

163 in table A.1 of Appendix A. The trees were also chosen within the different diameter classes  
164 based on the corresponding percentile values as this was described above. The *A. alba* trees  
165 were cut in February 2014 and the *Ps. menziesii* trees were cut in March 2015.

166 All the *Ps. menziesii* plots were issued from even aged plantations. The *A. alba* plots  
167 being issued from naturally generated forests, the age of the trees was estimated using an  
168 additional disc taken at the stump.

169 Table A.2 of Appendix A provides dendrometric variables about the trees.

## 170 2.2. Wood density measurement

171 The discs were X-ray scanned in a green state with a medical computed tomograph (CT)  
172 scanner. The discs were then dried in an oven at 103 °C to a constant weight. They were  
173 scanned again in the oven-dried state. More information about the wood density measure-  
174 ments by CT scanning is available in Freyburger et al. (2009).

175 Basic density (*BD*) of wood was computed for each disc from the two scans (in green and  
176 oven-dried states) as described in Longuetaud et al. (2016).

## 177 2.3. Calculation of variables

178 The relative height  $hr_{ij}$  of disc  $j$  from tree  $i$  is calculated as follows:

$$hr_{ij} = \frac{h_{ij}}{H_i}$$

179 with  $h_{ij}$  the height of disc  $j$  from tree  $i$  and  $H_i$  the total height of tree  $i$ .

180 The mean ring width at breast height  $RW130_i$  from tree  $i$  is estimated as follows, con-  
181 sidering the units of measurements given in table 2:

$$RW130_i = \frac{D130_i \cdot 10}{2 \cdot age_i}$$

182 with  $D130_i$  the diameter at breast height of tree  $i$  and  $age_i$  its age (actual or estimated).

183 The mean *BD* of stem wood for tree  $i$  is calculated from the mean *BD* of each disc  $j$   
184 from the tree  $i$  weighted by the volumes of wood of the stem short logs represented by each  
185 disc, i.e. a portion of the stem on either side of the disc calculated so that each part of the  
186 stem is associated with the closest disc.

187 *2.4. Statistical modelling*

188 The R software was used for statistical analyses (R Core Team, 2020). The main functions  
189 used were: the `lm`, `nls`, `anova`, `AIC` and `TukeyHSD` functions from the `stats` package and the  
190 `nlsList`, `nlme`, `gnls` and `ACF` functions from the `nlme` package.

191 In each case, for our vertical profiles of  $BD$ , mixed-effect models were fitted to obtain  
192 for each tree the best set of parameters and then to assess step by step the predictive power  
193 of thinning modality and tree variables on those model parameters. When required, an  
194 autoregressive correlation structure of order 1 (`corAR1`) was used to take into account the  
195 correlation of within-group errors related to the multiple  $BD$  observations done along the  
196 stem of a given tree (Pinheiro and Bates, 2000).

197 Multiple linear regressions were also fitted at the disc level in order to predict  $BD$  from  
198 mean ring width and mean cambial age whatever the height in the tree. These regressions  
199 were fitted for comparison purpose with the previous models for vertical  $BD$  profiles, espe-  
200 cially with the models that take as input only external variables that are easily measurable  
201 in the forest. As density models as a function of ring width and cambial age are usually  
202 developed at the annual ring level, we also tried to calculate mean ring width and mean  
203 cambial age by weighting by the area of each ring to be more representative of the disc.

204 For comparison with other models from the literature, RMSE, relative RMSE and AIC  
205 were used. The models from the literature have been fitted on our data set. The models  
206 were then compared on the basis of their fixed-effects only ( $b_0, \dots, b_5$  in Table 1).

207 Since most of the vertical density profiles had a U-shape pattern, we chose a biexponen-  
208 tial model as described by Crawley (2012) rather than a polynomial model. Most of the  
209 approaches found in the literature are based on polynomial models. We made the hypothesis  
210 that the biexponential model is more robust and that the parameters are easier to interpret  
211 because they are less correlated than in a polynomial model.

212 The general form of the model is given in Equation 1:

$$BD_j = f(hr_j) = a \cdot \exp(b \cdot hr_j) + c \cdot \exp(d \cdot hr_j) \quad (1)$$

213 with  $BD_j$  the basic density of disc  $j$  (in  $\text{kg} \cdot \text{m}^{-3}$ ) at the relative height  $h_j$  and  $a$ ,  $b$ ,  $c$  and  
214  $d$  the model parameters.

215 At the ground level, the  $BD$  predicted by model (1) is:

$$f(0) = a + c = k \quad (2)$$

216 It is thus expected to have a relationship between  $k$  and the  $BD$  at breast height ( $BD130$ ).

217 By replacing  $a$  by  $k - c$  and factoring by  $c$  in Equation 1, we obtained:

$$BD_j = c \cdot (\exp(d \cdot hr_j) - \exp(b \cdot hr_j)) + k \cdot \exp(b \cdot hr_j) \quad (3)$$

218 For each species, two models derived from Equation 3 were tested: A first model not  
219 using  $BD130$  as input variable (model called NBD) and a second one with  $BD130$  as input  
220 variable (model called WBD). The reason for distinguishing both cases is that, as it will be  
221 shown,  $BD130$  considerably helps to predict the  $BD$  profile, but is rarely measured in the  
222 field. The interest of WBD model is that it could take as input the output of a  $BD130$   
223 model that would be developed on a larger number of trees and that would take into account  
224 tree variables and ecological characteristics at the resource scale. This is one objective of the  
225 XyloDensMap project for instance (Jacquin et al., 2019).

226 Apart from  $BD130$ , the other candidate explanatory variables tested in our models were:  
227 the relative height of the disc ( $hr$ ), the circumference at breast height ( $C130$ ), the total tree  
228 height ( $H$ ), the height to the base of the living crown ( $hLC$ ), the relative height to the base  
229 of the living crown ( $hrLC$ ), the ratio height/diameter ( $\frac{H}{D130}$ ), the tree age ( $age$ ) and the  
230 mean annual ring width at breast height ( $RW130$ ).

231 Other vertical profile models in which a minimum of basic density was imposed at the  
232 height of the base of the living crown were tested. But these models were too constrained  
233 and less efficient.

234 Mixed models were fitted on all trees at once by testing random effects on each parameters  
235 for each species, resulting in a set of parameters  $k$ ,  $b$ ,  $c$  and  $d$  for each tree. By analysing  
236 the relations of  $k$ ,  $b$ ,  $c$ ,  $d$  with the tree descriptors (avoiding to use in the same equations  
237 correlated variables), several relations were obtained for several parameters (see section 3.5).  
238 We therefore introduced these relations in the general models to verify, for each species, if  
239 random tree effect parameters were still necessary.

240 *2.4.1. Model without basic density at breast height (NBD)*

241 For this model, Equation 3 was used as is for calibration and search for explanatory  
242 variables.

243 *2.4.2. Model including basic density at breast height (WBD)*

244 By forcing the model to pass through  $BD_{130}$  at 1.30 it was possible to remove one  
245 parameter from the model. Indeed, for  $hr_j = 1.30/H$  in Equation 3, it is possible to express  
246  $c$  as:

$$c = \frac{BD_{130} - k \cdot \exp(b \cdot \frac{1.30}{H})}{\exp(d \cdot \frac{1.30}{H}) - \exp(b \cdot \frac{1.30}{H})} \quad (4)$$

247 Then, replacing  $c$  in Equation 3, we obtain:

$$BD_j = \frac{BD_{130} - k \cdot \exp(b \cdot \frac{1.30}{H})}{\exp(d \cdot \frac{1.30}{H}) - \exp(b \cdot \frac{1.30}{H})} \cdot (\exp(d \cdot hr_j) - \exp(b \cdot hr_j)) + k \cdot \exp(b \cdot hr_j) \quad (5)$$

248 where  $b$ ,  $d$  and  $k$  are the model parameters

249 For comparison with the WBD models, the Kimberley models were tested by replacing  
250 in the equations the breast height 1.4 m by 1.3 m in our study.

251 **3. Results**

252 *3.1. Relationship between thinning intensity and the measured variables*

253 *3.1.1. Dendrometric variables*

254 By plotting boxplots of tree related variables for each plot (Appendix B), it can be verified  
255 that the measured dendrometric variables were well adapted to characterize the effect of  
256 thinning intensities.

257 *3.1.2. Basic density*

258  $BD_{130}$  did not seem to highly depend on the thinning intensity, except maybe for the  
259 mature stands of *Ps. menziesii* (variation significant only for forest Pm2). While for *A.*  
260 *alba*  $BD_{130}$  seemed to be higher in the unthinned stand of forest Aa3 (even if the difference  
261 was not significant), for *Ps. menziesii*  $BD_{130}$  tended to be lower in the unthinned mature  
262 stands.

263 For the mean  $BD$  of the stem, the difference between thinning intensities was statistically  
 264 significant for stands Aa1 and Pm2. For these two forests, it was clear that  $BD$  was higher  
 265 in heavy thinning modalities. Even if the results were not significant, we observed the same  
 266 tendencies for the other forests with less important differences and with the exception of Aa3  
 267 and Pm3.

268 *3.2. Basic density at breast height versus mean basic density of the stem wood*

269 Breast height is the reference height for many measurements (diameter, ring width, den-  
 270 sity...). In a first analysis, the mean  $BD$  of the whole stem was compared with the mean  $BD$   
 271 of the disc taken at breast height (Figure 1). A paired t-test was applied (Table 4). This  
 272 part of the work is a continuation of the work done previously in Longuetaud et al. (2017).

273 Table 4 shows that the mean  $BD$  of the stem is significantly different from that at breast  
 274 height for *A. alba* and *Ps. menziesii*. The  $BD$  at breast height is generally higher than the  
 275 mean  $BD$  of the stem. Results were the same regardless of the data source.

Table 4: Mean basic density of the whole stem wood and mean basic density of the disc at breast height. The symbols indicate the significance of the difference based on a paired t-test: NS:  $p \geq 0.05$ , \*:  $p < 0.05$ , \*\*:  $p < 0.01$ , \*\*\*:  $p < 0.001$ .

Tree species	Number of trees	Mean $BD$	Mean $BD$	Difference between $BD$ at breast height	Significance of the difference
		at breast height ( $\text{kg} \cdot \text{m}^{-3}$ )	of the stem wood ( $\text{kg} \cdot \text{m}^{-3}$ )	and mean $BD$ of the stem wood ( $\text{kg} \cdot \text{m}^{-3}$ )	
<i>A. alba</i>	37	378.80	358.24	20.56	***
<i>Ps. menziessii</i>	36	445.74	423.03	21.45	***

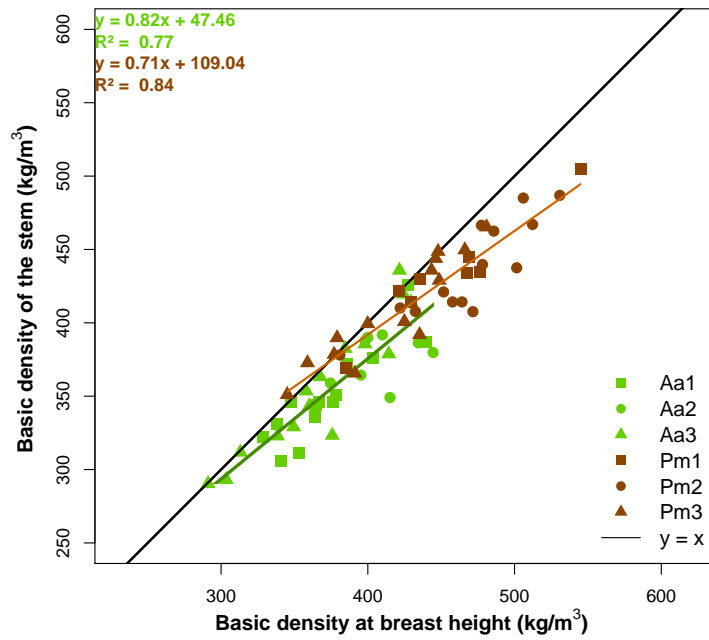


Figure 1: Mean basic density of the whole stem wood as a function of the mean basic density of the breast height disc for each species and each stand (refer to Table 3 for the meaning of the abbreviations in the legend). The black line is the  $y=x$  line. The green line is the linear regression for *A. alba* and the brown one the linear regression for *Ps. menziesii*. The regression equations and the coefficients of determination for each species are given in the same colors as the points.

276 3.3. Basic density of a disc versus ring width and cambial age

277 When considering the whole sample for each species, there was no clear relationship  
278 between  $BD$  and ring width at the disc level, with  $R^2$  ranging from 0.01 to 0.14 depending  
279 on the species (Figure 2). Considering that each ring should contribute to the disc  $BD$   
280 in proportion to its area we have also tried to relate  $BD$  of discs to the mean ring width  
281 weighted by ring areas: The results were not much better (Figure C.1 in Appendix C).

282  $BD$  was slightly more correlated with the mean cambial age (*i.e.* half the number of rings  
283 in the disc), especially for *Ps. menziesii* with  $R^2$  from 0.12 to 0.17 (Figure 2). The mean  
284 cambial age weighted by ring areas was not more correlated to the disc  $BD$  (Figure C.1 in  
285 Appendix C).

286 Multiple linear regressions were fitted with mean ring width, mean cambial age and  
287 interaction between the two variables as explanatory variables. For comparison purpose,  
288 AIC, RMSE and relative RMSE are given in Table 7.

289 3.4. Variation of basic density along the stem

290 The variation of  $BD$  with height (Appendix D) shows that for *A. alba*, the variation  
291 seemed to be strong for unthinned plots with a high  $BD$  at the bottom of the tree. Variation  
292 was lower for heavy thinning plots and the  $BD$  at the bottom of the tree was lower than that  
293 of trees from unthinned plots.

294 For *Ps. menziesii*, it was the opposite (Appendix E). The variation was higher for heavy  
295 thinning plots and lower for unthinned plots. This time, the  $BD$  at the bottom of the tree was  
296 higher for heavy thinning plots than for unthinned plots. This observation is not applicable  
297 to stand Pm3 in which the trees were the youngest (20 years) and the variations in  $BD$  were  
298 quite low.

299 For both species,  $BD$  decreased as the height in the stem increased.

300 Figures 3, 4 and 5 show that the models manage to express well the variability at the  
301 bottom of the trees.



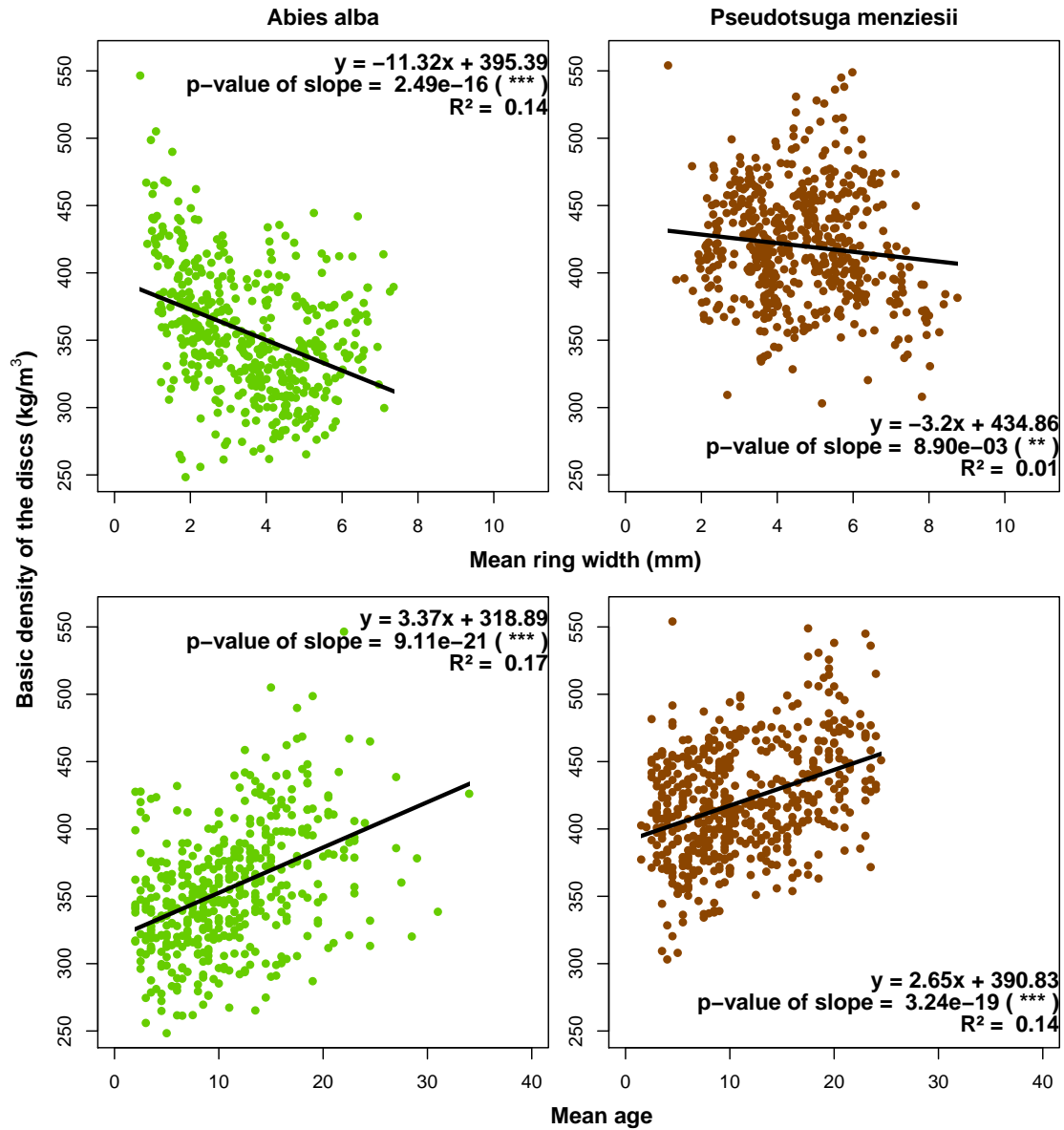


Figure 2: Mean basic density as a function of ring width and cambial age at the disc level. The black lines correspond to the regression lines. The regression equations and the significance of the slope parameters (p-values) are given on each plot: NS:  $p \geq 0.05$ , \*:  $p < 0.05$ , \*\*:  $p < 0.01$ , \*\*\*:  $p < 0.001$ .

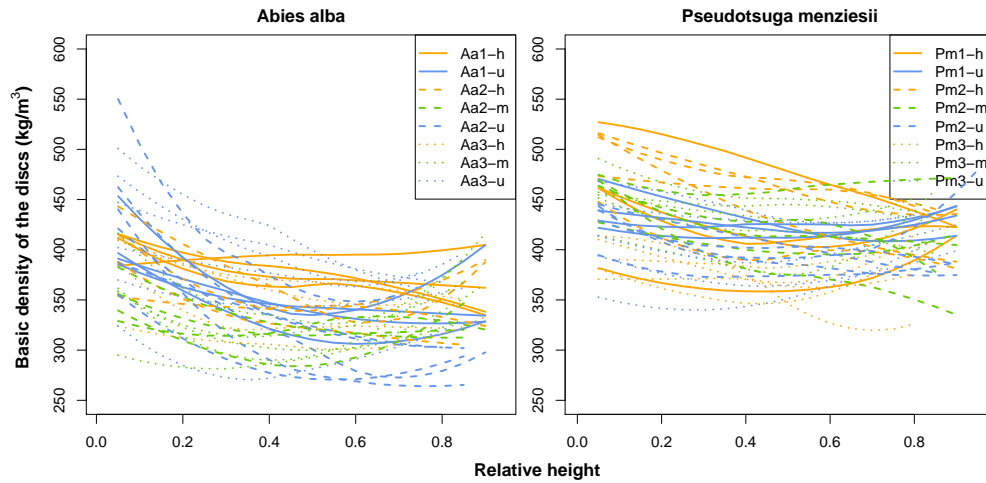


Figure 3: Smoothed curves of basic density variation with relative height for all the trees for each species. The colors represent the thinning intensities: Orange is for trees from the heavy thinning plots, green for trees from moderate thinning plots and blue for trees from plots without thinning. The line type identifies the stand.

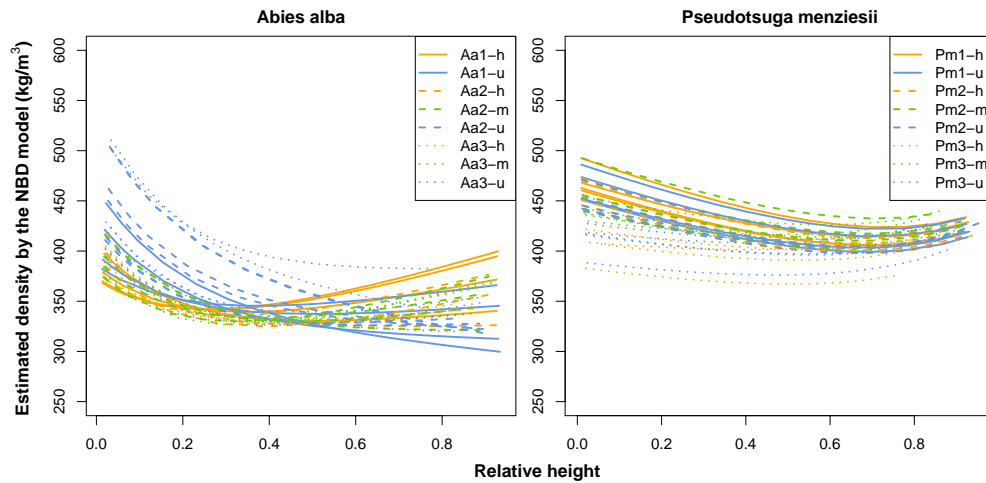


Figure 4: Profiles of basic density estimated by the NBD models for each tree (*A. alba* and *Ps. menziesii*). The colors represent thinning: Orange is for the trees from the heavy thinning plots, green is for the trees from the moderate thinning plots and blue is for the trees from without thinning plots. The line type identifies the stand.

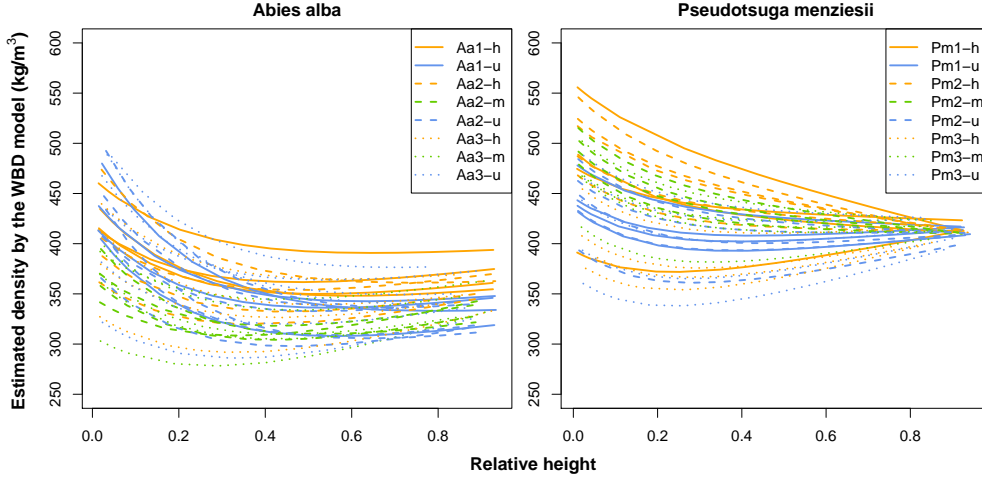


Figure 5: Profiles of basic density estimated by the WBD models for each tree (*A. alba* and *Ps. menziesii*). The colors represent thinning: Orange is for the trees from the heavy thinning plots, green is for the trees from the moderate thinning plots and blue is for the trees from without thinning plots. The line type identifies the stand.

### 3.5. Vertical profile models without basic density at breast height (NBD)

Table 7 gives the values of absolute and relative RMSE (by using the fixed-effects only) and AIC obtained with our model and models from literature that do not include  $BD_{130}$ . All the models were calibrated on our data set for comparison purpose. For the Deng et al. (2014) model, we used a diagonal variance-covariance matrix for the random-effect parameters otherwise it was not possible to obtain the convergence of the model.

#### 3.5.1. *A. alba*

For the model without  $BD_{130}$  as input variable, we obtained for *A. alba* the following modeling of the initial parameters as a function of tree variables:

$$\begin{cases} k_i = k_1 \cdot \frac{1}{C_{130_i}} + k_2 + \alpha_i \\ b_i = b_1 \cdot \frac{H_i}{D_{130_i}} + b_2 + \beta_i \\ c_i = c_1 \cdot H_i + c_2 + \gamma_i \end{cases} \quad (6)$$

Random-effect parameters  $\alpha_i$ ,  $\beta_i$  and  $\gamma_i$  were needed for  $k_2$ ,  $b_2$  and  $c_2$ , respectively, and were kept in the final model.

313 Since no relation was obtained for parameter  $d$ , it was let as is in the general model.  
 314 Table 5 gives the values of the fixed-effect parameters for the final mixed-effect model. The  
 315 standard deviations of random-effect parameters  $\alpha_i$ ,  $\beta_i$  and  $\gamma_i$  were 3.29e+01, 2.22e-01 and  
 316 5.06e+01, respectively.

Table 5: Fixed-effect parameters and their standard deviations (in brackets) for the NBD model not using basic density at breast height for *A. alba*.

Species	$k_1$	$k_2$	$b_1$	$b_2$	$c_1$	$c_2$	$d$
<i>A. alba</i>	3.890985e+03	3.421220e+02	-5.849102e-03	6.240366e-01	-5.648390e+00	1.966764e+02	-5.160087e+00
	(5.056307e+02)	(1.188139e+01)	(9.198257e-04)	(9.707743e-02)	(1.500177e+00)	(2.595777e+01)	(7.320403e-01)

### 317 3.5.2. *Ps. menziesii*

318 We obtained for *Ps. menziesii* the following model of the initial parameters as a function  
 319 of tree variables:

$$\left\{ \begin{array}{l} k_i = k_1 \cdot \frac{1}{H_i} + k_2 \cdot RW130 + k_3 \cdot hrLC_i + k_4 + \alpha_i \\ b_i = k \cdot (b_1 \cdot \frac{1}{H_i} + b_2 + \beta_i) \end{array} \right. \quad (7)$$

320 The analysis showed that random-effect parameters  $\alpha_i$  and  $\beta_i$  were needed for  $k_4$  and  $b_2$   
 321 respectively in the final model. Since no relation were obtained for parameters  $d$  and  $c$ , there  
 322 were let as is in the general model. Table 6 gives the values of the fixed-effect parameters of  
 323 the final mixed-effect model. The standard deviations of random-effect parameters  $\alpha_i$  and  $\beta_i$   
 324 were 3.65e+01 and 1.93e-04, respectively.

325 The plots of  $BD$  predicted by the different models as a function of the relative height in  
 326 the tree are presented in Appendices D and E.

Table 6: Fixed-effect parameters and their standard deviations (in brackets) for the NBD model not using basic density at breast height for *Ps. menziesii*.

Species	$k_1$	$k_2$	$k_3$	$k_4$	$b_1$	$b_2$	$c$	$d$
<i>Ps. menziesii</i>	-1.842987e+03	-1.828230e+01	-1.494966e+02	6.978071e+02	5.841137e-03	-8.275563e-04	2.996460e+00	3.411697e+00
	(4.272549e+02)	(6.591333e+00)	(5.491386e+01)	(7.067386e+01)	(1.875783e-03)	(1.398871e-04)	(4.052021e+00)	(1.205966e+00)

Table 7: AIC, RMSE and relative RMSE for the NBD models and various models from the literature not using basic density at breast height.

Tree species	Model	Number of parameters	AIC	RMSE (kg · m <sup>-3</sup> )	Relative RMSE (%)
<i>Abies alba</i>	NBD	7	4230.29	35.29	9.92
	Multiple regression at disc level	4	4717.58	40.82	11.47
	Repola (2006)	5	4256.82	40.90	11.50
	González-Rodrigo et al. (2013)	2	4785.11	44.13	12.40
	Deng et al. (2014)	6	4305.45	46.76	13.14
<i>Pseudotsuga menziesii</i>	NBD	8	4571.37	34.19	8.11
	Multiple regression at disc level	4	5097.03	38.01	9.01
	Repola (2006)	5	4544.92	37.64	8.93
	González-Rodrigo et al. (2013)	2	5155.69	40.45	9.59
	Deng et al. (2014)	6	4568.35	37.98	9.01

### 3.6. Vertical profile models with basic density at breast height (WBD)

Table 10 gives the values of AIC, RMSE and relative RMSE (by using the fixed-effects only) obtained with our model and Kimberley et al. (2015) model which was calibrated on our data set for comparison purpose.

#### 3.6.1. *A. alba*

For the WBD model, we obtained for *A. alba* the following models of the initial parameters as a function of tree variables:

$$\begin{cases} k_i = (k_1 \cdot \frac{1}{C_{130_i}} + k_2 + \alpha_i) \cdot BD_{130_i} \\ d_i = d_1 \cdot \frac{1}{BD_{130_i}} + d_2 + \beta_i \end{cases} \quad (8)$$

Random-effect parameters  $\alpha_i$  and  $\beta_i$  were needed for  $k_2$  and  $d_2$  respectively and a diagonal variance-covariance matrix was used. An autoregressive correlation structure of order 1 was used. The single correlation parameter was 2.39e-01.

Since no relation was obtained for parameter  $b$ , it was let as is in the general model. Table 8 gives the values of the fixed-effect parameters for the final mixed-effect model. The standard deviations of random-effect parameters  $\alpha_i$  and  $\beta_i$  were 2.57e-02 and 1.26e-01, respectively.

#### 3.6.2. *Ps. menziesii*

We obtained for *Ps. menziesii* the following modeling of the initial parameters as a function of tree variables:

$$\begin{cases} k_i = (k_1 \cdot H_i + k_2) \cdot BD130_i \\ d_i = (d_1 + \alpha_i) \cdot BD130_i + d_2 \end{cases} \quad (9)$$

343 Since no relation was obtained for parameter  $b$ , it was let as is in the general model.  
 344 Random-effect parameter  $\alpha_i$  was needed for  $d1$ . An autoregressive correlation structure of  
 345 order 1 was used. The single correlation parameter was 2.10e-01.

346 Table 9 gives the values of the fixed-effect parameters for the final mixed-effect model.  
 347 The standard deviation of random-effect parameter  $\alpha_i$  was 2.22e-04.

Table 8: Fixed-effect parameters and their standard deviations (in brackets) for the WBD model with basic density at breast height for *A. alba*.

Species	$k_1$	$k_2$	$b$	$d_1$	$d_2$
<i>A. alba</i>	4.2497463e+00 (6.484259e-01)	1.0127349e+00 (1.178484e-02)	-4.3583799e+00 (5.784795e-01)	2.962377782e+02 (1.025718e+02)	-6.015024e-01 (2.801850e-01)

Table 9: Fixed-effect parameters and their standard deviations (in brackets) for the WBD model with basic density at breast height for *Ps. menziesii*.

Species	$k_1$	$k_2$	$b$	$d_1$	$d_2$
<i>Ps. menziesii</i>	-2.097975e-03 (5.025279e-04)	1.090797856e+00 (1.708982e-02)	-6.142812835e+00 (1.332227e+00)	-2.819938e-03 (4.137676e-04)	1.285744246e+00 (1.928312e-01)

Table 10: AIC, RMSE and relative RMSE for the WBD models and various models from the literature with basic density at breast height.

Tree species	Model	Number of parameters	AIC	RMSE (kg · m <sup>-3</sup> )	Relative RMSE (%)
	WBD	6	4250.76	27.09	7.62
<i>A. alba</i>	Kimberley et al. (2015)	5	4402.06	28.88	8.12
	Kimberley et al. (2017)	3	4532.56	33.44	9.40
	WBD	6	4529.57	24.83	5.89
<i>Ps. menziesii</i>	Kimberley et al. (2015)	5	4679.22	25.04	5.94
	Kimberley et al. (2017)	3	4938.27	32.52	7.71

348 The graphs representing the  $BD$  predicted by the different models as a function of the  
 349 relative height in the tree are given in Appendices D and E.

### 350 3.7. Relevance of the models

351 In the models based on Equation 3, the parameter  $k$  represents the  $BD$  at the ground  
352 level. For *A. alba* this parameter was controlled by tree size since  $k$  increased when  $C130$   
353 decreased in the NBD model. For the WBD model, the same trend was observed. Thus,  
354 smaller trees would have higher  $BD$  at the bottom of the stem.

355 For *Ps. menziesii* the parameter  $k$  of the NBD model was found to be related to  $H$ ,  
356  $RW130$  and  $hrLC$ . Considering the values of the corresponding parameters it appears that,  
357 here also  $k$  increased when ring width decreased. In addition, more the tree was small in  
358 height, lower dense it was at the ground level (e.g., a 20 m high tree is  $18 \text{ kg.m}^{-3}$  less dense  
359 than a tree of 25 m high tree). For the WBD model, a large part of the variation between trees  
360 was already taken into account through the variable  $BD130$ , which could explain that the  
361 effect of  $H$  on  $k$  was weaker than above and not in the same direction (e.g.,  $k = 1.05 \cdot BD130$   
362 for a 20 m height tree versus  $1.04 \cdot BD130$  for a 25 m height tree).

363 The parameters  $b$  and  $d$  controlled the slopes of the  $BD$  variation in the stem and were  
364 more difficult to interpret since both effects can add up or offset each other to a certain  
365 extent. For the models including  $BD130$ ,  $b$  was negative for both species with a relatively  
366 constant value for all trees of a given species (no random effect). The decrease seemed strong  
367 for both species (Appendices D and E).

368 On the other hand, the parameter  $d$  was dependent on  $BD130$ . When  $BD130$  increased,  
369 the value of  $d$  decreased and even became negative for *Ps. menziesii* (e.g., for *A. alba*,  
370  $d = 0.39$  for  $BD130 = 300 \text{ kg.m}^{-3}$  and  $d = 0.14$  for  $BD130 = 400 \text{ kg.m}^{-3}$ , and for *Ps.*  
371 *menziesii*,  $d = 0.16$  for  $BD130 = 400 \text{ kg.m}^{-3}$  and  $d = -0.12$  for  $BD130 = 500 \text{ kg.m}^{-3}$ ).

## 372 4. Discussion

### 373 4.1. Two very different softwood species

374 Firstly, these species are ecologically very different with contrasted strategies. *A. alba*  
375 is a shade-tolerant and late-successional species with a shade-tolerance score of  $4.60 (0.06)$ <sup>1</sup>

---

<sup>1</sup>Shade-tolerance score and standard deviation in brackets. Tolerance scores range from 0 (no tolerance) to 5 (maximal tolerance).

376 (Niinemets and Valladares, 2006) and is known to have a very slow radial growth in the early  
377 years. At the opposite, *Ps. menziesii* is rather shade-intolerant with a score of 2.78 (0.18).

378 From an anatomical point of view these species are also different. *A. alba* shows a pro-  
379 gressive transition between earlywood and latewood while *Ps. menziesii* shows an abrupt  
380 transition. Todaro and Macchioni (2011) suggest that there is a link between these anatom-  
381 ical characteristics and the presence of a negative correlation between ring wood density  
382 and ring width. This negative correlation is often reported for *P. abies* but the results are  
383 sometimes controversial, especially for *Ps. menziesii* (Jozsa et al., 1994).

#### 384 4.2. Factors that influence wood density and its vertical variation in the stem

385 The observed patterns of vertical variation in *BD* were the following. For *A. alba*, *BD*  
386 tended to decrease from the butt to the height of the living crown then sometimes to increase  
387 towards the top (U-shape). For *Ps. menziesii*, *BD* decreased from the butt to the top of  
388 the stem for most of the trees. A few trees followed the opposite trend. *Ps. menziesii* and  
389 *A. alba* were few studied for their vertical variation in density. On *Ps. menziesii*, Kimberley  
390 et al. (2017) found a sigmoidal pattern with an increase in density towards the bottom of  
391 the stem and a decrease towards the top which is in overall consistent with our observations,  
392 except maybe towards the top of the stem. On *A. alba*, González-Rodrigo et al. (2013) used  
393 a linear model to describe the decrease in wood density with height in the stems.

394 To try to explain these vertical variations we can return to the more widely studied radial  
395 variations. Indeed, radial variations in density can have an impact on vertical variations in  
396 the stem, as the proportions (of the wood disc area) of different types of wood (e.g., juvenile  
397 *versus* mature wood), or the proportion of narrow rings, for instance, can change with the  
398 height in the tree.

##### 399 4.2.1. The juvenile wood

400 For Lachenbruch et al. (2011), the typical radial pattern for the wood density of most  
401 softwood species is to have a corewood with a lower density than the outerwood. Wood-  
402 cock and Shier (2002) highlighted the relationship between such radial patterns and species  
403 strategies. In Longuetaud et al. (2017), less dense wood was observed in about the first five  
404 cm around the pith for *Ps. menziesii* followed by an increase in *BD* with a sigmoid pattern.



405 While for *A. alba* a progressive decrease in  $BD$  from the centre of the stem was observed in  
406 this previous study. This was consistent with the successional status of these two species. As  
407 reported by Lachenbruch et al. (2011), the amount of corewood varies with the height in the  
408 stem. As a consequence, for species showing a strong difference in density between juvenile  
409 and mature wood, it is automatic that a variation of density with height is observed due to  
410 the variation with height of the proportion of juvenile wood which increases from the base  
411 to the top of the tree (Zobel and Van Buijtenen, 1989). From these considerations we could  
412 expect a higher  $BD$ , at least for *Ps. menziesii*, at the bottom of the stem than at the top,  
413 which was generally the case on our trees.

414 From the literature (Zobel and Van Buijtenen, 1989; Henin et al., 2018; Fabris, 2000),  
415 the effect of the proportion of juvenile wood on the wood density at a given height level is  
416 clear, as well as the effect on the variations in density with height. For a given tree, in our  
417 data, the proportion of juvenile wood increased from the bottom to the top of the stem and  
418 it contributes to explain at least partially the vertical variations in  $BD$ . Thus hypothesis **H1**  
419 seems to be verified.

#### 420 4.2.2. *The growth rate*

421 The well-known negative correlation between ring density and ring width has been ob-  
422 served and extensively studied especially on *Picea* spp. (e.g., Bouriaud et al., 2015). The  
423 few studies related to this relationship on *A. alba* (Hamada et al., 2018; Sopushynskyy et al.,  
424 2020) lead to believe that this species behaves in the same way that *P. abies*. On the contrary,  
425 according to Jozsa and Brix (1989) and Fabris (2000), the growth rate has little impact on  
426 the whole-ring density for *Ps. menziesii*.

427 These results were confirmed by our study which shows a decrease of the whole disc  
428  $BD$  with the increase of the average ring width for *A. alba* and a weaker but significant  
429 relationship for *Ps. menziesii*. If we refer to the Pressler's law, the rings are wider at the top  
430 of the stem (Pressler, 1864; Cortini et al., 2013) and this should lead to have a higher  $BD$   
431 at the bottom of the stem than at the top, at least for *A. alba*. It was generally the case for  
432 our trees.

433 With respect to the hypothesis **H2**, the regression of the disc  $BD$  as a function of the

434 corresponding mean ring width was significant for both species although very weak for *Ps.*  
435 *menziesii* but this relationship was not sufficient to explain the observed *BD* variations in  
436 the stem. For *Ps. menziesii*, it was quite clear that a dynamic growth rate had not the  
437 expected negative effect on the wood density at the disc or stem levels.

#### 438 4.2.3. *The cambial age*

439 For *Ps. menziesii*, Fabris (2000) has reported that radial variations in density are mainly  
440 due to variations in cambial age. Filipescu et al. (2014) on the same species have described a  
441 radial increase in density as a function of cambial age. These results were confirmed by our  
442 study which shows an increase in disc *BD* with increasing cambial age for *Ps. menziesii*. For  
443 *A. alba*, we observed the same behaviour while the results of Hamada et al. (2018), concerning  
444 only four trees, do not show a clear trend of ring density with cambial age at breast height.  
445 For both species the relationship between whole disc *BD* and cambial age was stronger than  
446 the aforementioned potential relationship between density and average ring width. Indeed,  
447 it is difficult to separate the two effects and, as pointed out by Jozsa et al. (1994), the true  
448 effect of growth rate on annual ring wood density should be studied for comparable cambial  
449 ages. Finally, as the number of rings decreases from the base to the top of the tree, we could  
450 expect a higher *BD* at the bottom of the stem than at the top, which was generally the case  
451 on our trees.

452 Despite the observed relationships of *BD* with ring width and age, the multiple linear  
453 regressions that were tested at the disc level to explain the vertical variations of *BD* from  
454 these variables only were clearly less efficient than our NBD models. It probably means  
455 that the vertical variations in *BD* were also due to other variables such as the proportion of  
456 juvenile wood (Section 4.2.1).

#### 457 4.2.4. *The compression wood*

458 The reaction wood, called compression wood (*CW*) for softwood species, has an impact on  
459 density. It has already been shown that *CW* is denser than normal wood (Pillow and Luxford,  
460 1937; Harris, 1977; Gryc and Horáček, 2007; Tarmian et al., 2012) because it is characterized  
461 by cells with large walls (Li et al., 2014) and wide rings with a high proportion of latewood  
462 (Lee and Eom, 1988). *CW* can be found all along the stem, even in small quantities, because

463 the tree must be able to face the wind, to restore vertical growth (gravitropy), to incline  
464 stems (e.g., heliotropy) (Barnett et al., 2014). It is more generally located along limited  
465 portions of the stem except for a relatively straight and vertical tree becoming inclined for  
466 its entire length, for which *CW* can be found all along the stem (Pillow and Luxford, 1937).

467 The amount of *CW* is often more important in the lower part of the stem (Pillow and  
468 Luxford, 1937; Westing, 1965; Donaldson et al., 2004).

469 The greater presence of *CW* at the bottom of the stem may also explain the higher *BD*  
470 in this part, especially since some of our plots were located on slopes.

#### 471 4.2.5. *The thinning intensity*

472 The thinning intensity makes it possible to modulate the growth rate which we have  
473 already discussed above. However, we could not say whether the observed *BD* variations,  
474 especially regarding vertical patterns, were related to a difference in growth rate or tree size.

475 In overall, for *A. alba*, a steeper decreasing slope of *BD* from the base of the stem was  
476 observed in the unthinned plots. Conversely, for *Ps. menziesii*, steeper decreasing slope  
477 from the base of the stem was rather observed in thinned stands while trees from unthinned  
478 stands showed more constant patterns. It could be expected that the most cylindrical trees,  
479 i.e. those of the unthinned stands, show more variability between the bottom and the top of  
480 the stem because it is known that in case of unfavourable conditions for growth the annual  
481 increase is more strongly reduced at the bottom than at the top (Courbet, 1999). This would  
482 be consistent with what was observed for *A. alba*. Sometimes the difference observed between  
483 trees could also be explained by a steeper local slope in the field leading to the formation of  
484 *CW*.

485 An original and unexpected result was the observation of a higher *BD* of discs in average  
486 (i.e., at disc and stem levels) for the heavier thinning intensities in one mature stand of *Ps.*  
487 *menziesii* and one of *A. alba*, while there was no effect of the thinning intensity for the other  
488 stands. Intuitively, one would tend to think that trees from dense stands will have denser  
489 wood. In general, a higher *BD* is expected for slow-growing softwood trees with narrow  
490 ring widths, i.e., in the unthinned modalities, due to the well-known relationship between  
491 ring width, proportion of latewood and wood density (see also Section 4.2.2). Moreover,

492 according to Pillow and Luxford (1937), young trees having their crown free from competition  
493 have smaller  $CW$  rate than young trees grown in dense stands, which should contribute to  
494 increase density in the unthinned modalities. Nevertheless, the opposite was observed.

495 As pointed out by Fabris (2000) for *Ps. menziesii*, for sufficiently long rotation periods,  
496 trees with high growth rate will have lower proportion of juvenile wood than slow-growing  
497 trees. In his work, the growth rate was mainly modulated by initial spacing while in our  
498 study the thinning intensity was the main studied factor. A lower proportion of juvenile  
499 wood in the thinned stands could explain at least partially the observed differences in  $BD$ .

500 In our case, the surface of the first inner rings was in average clearly lower in the trees  
501 from the unthinned stands (Figure F.3 in Appendix F) may be due to uncontrolled factors  
502 (genetic, juvenile wood definition). Despite this, it appeared that for most stands, except Aa1  
503 and Pm1, the proportion of juvenile wood was finally higher in the trees from the unthinned  
504 modality (Figure F.2 in Appendix F), tending to confirm the above explanation of Fabris  
505 (2000).

506 If the  $BD$  radial variation is mainly due to cambial age and to the juvenile or mature  
507 nature of wood (hypothesis **H1**) there would be an interest in making the trees grow faster in  
508 order to decrease the proportion of juvenile wood. This is not inconsistent with the advice of  
509 Henin et al. (2018), for minimising the proportion of juvenile wood, to maintain high stand  
510 density in the initial phase of growth.

511 As a result, the average  $BD$  of the fast-growing trees from heavily thinned stands would  
512 be higher since juvenile wood or more generally corewood is known to be of lower density  
513 for most softwood (Lachenbruch et al., 2011). Moreover, the annual rings corresponding to  
514 the highest cambial ages and therefore the densest ones will represent a larger surface in  
515 fast-growing trees. On the other hand, Todaro and Macchioni (2011) found a higher  $BD$   
516 in unthinned stands of young 31-year-old *Ps. menziesii* trees. For our 20-year-old trees of  
517 stand Pm3, the results were more or less similar with lower  $BD$  in the heavily thinned plot  
518 than in the unthinned one.

519 Finally, hypothesis **H3** seems verified. Indeed, the effects of thinning intensity on growth  
520 rate, tree size and therefore on the variations of juvenile wood proportions are reflected, but  
521 in a complex way, on the vertical variations in  $BD$ .

### 522 4.3. Representativeness of breast height measurements

523 In analogy to the radial patterns of density variation and their relationship with species  
524 strategies proposed in the literature (Plourde et al., 2015; Woodcock and Shier, 2002), we  
525 can propose a similar rule for vertical variations, that would rather be associated with the  
526 strategy of the tree according to its growing conditions. In Figure 3, 4 and 5, and in a very  
527 schematic way, it can be observed that trees with the lowest  $BD$  at 1.30 m tend to show an  
528 increase with height while those with the highest  $BD$  at 1.30 m tend to show a decrease with  
529 height.

530 The results obtained in Longuetaud et al. (2017) were confirmed with the additional trees  
531 that were sampled in this extended study. The  $BD$  was significantly higher at 1.30 m than  
532 in average for the whole stem for *A. alba* and *Ps. menziesii*, which confirms hypothesis **H4**.  
533 Mitchell and Denne (1997) found the same results for *Picea sitchensis* and hypothesized that  
534 this difference can be explained by tracheids with wider walls at breast height. Wassenberg  
535 et al. (2015) have observed a higher density at the bottom of the stem for six species and  
536 raise the question of the best sampling strategy for density and biomass estimations. As  
537 explained in Section 4.2, several factors vary along the stem and could explain the higher  
538  $BD$  observed at the base of the stem and thus the difference in  $BD$  between 1.30 m and the  
539 whole stem: the proportion of juvenile wood, the mean ring width, the number of rings and  
540 the amount of  $CW$ .

## 541 5. Conclusion

542 Vertical variations of wood density in the stem have been little studied so far. Moreover,  
543 few species have been treated in the literature. Only one study providing a model at the disc  
544 level was found for *Ps. menziesii* and another one for *A. alba*. This study was exploratory  
545 and based on a limited number of trees due to the destructive sampling and time consum-  
546 ing measurements. The results have to be confirmed by further studies carried out on a  
547 larger number of trees, probably with a simplified measurement protocol based on the results  
548 obtained in this type of study.

549 It has been shown that the variation in wood density along the stem did not follow  
550 the same pattern for *A. alba* and *Ps. menziesii*. While the density of *Ps. menziesii* was

551 decreasing continuously from the bottom to the top of the stem, with for some trees an  
552 increase towards the top of the stem, that of *A. alba* presented generally a U-shape pattern  
553 with first a decrease followed by an increase in the upper part of the stem.

554 The thinning intensity had an impact on the slope of the decrease in *BD* at the bottom  
555 of the stem. *BD* decreased faster, as the height in the stem increased, in unthinned plots  
556 than in thinned ones for *A. alba* while it decreased faster for thinned plots than in unthinned  
557 ones for *Ps. menziesii*.

558 For these two species, the *BD* measured at breast height was not representative of the  
559 whole stem *BD* due to these vertical variations.

560 Two types of models, including or not including *BD* at breast height as an input, have  
561 been proposed for *A. alba* and *Ps. menziesii* in order to best represent the variation of *BD*  
562 with height as a function of tree growth related variables. A comparison with more traditional  
563 approaches, which are based on the well-known relationship for softwood species between  
564 annual ring density and both ring width and cambial age, have shown that our biexponential  
565 models using easily measurable external variables were relevant and gave better results to  
566 describe *BD* variations in the stem.

567 The continuation of this work will be to study the vertical variations in *BD* for the bark  
568 component and the variation in *BD* along the knot-branch continuum.

## 569 **Acknowledgements:**

570 A large part of the sampling used in this study was collected in the experimental network  
571 of Douglas stands managed by the *GIS Coop* (<https://www6.inrae.fr/giscoop> (Seynave et  
572 al. 2018). The authors would like to thank SILVATECH (Silvatech, INRAE, 2018. Structural  
573 and functional analysis of tree and wood Facility, doi: 10.15454/1.5572400113627854E12)  
574 from UMR 1434 SILVA, 1136 IAM, 1138 BEF and 4370 EA LERMAB EEF research center  
575 INRA Nancy-Lorraine for the realisation of X-ray tomograph observations. SILVATECH  
576 facility is supported by the French National Research Agency through the Laboratory of  
577 Excellence ARBRE (ANR-11-LABX-0002-01).

578 We would like to thank Vincent Rousselet, Frédéric Bordat, Loïc Dailly and Adrien Con-  
579 tini for the sampling in the forest and measurements at the laboratory and Charline Mola for

580 the CT scanner acquisitions. We are grateful to Adeline Motz and Daniel Rittié for the rings  
581 measures.

## 582 **Funding:**

583 SILVA laboratory is supported by a grant overseen by the French National Research  
584 Agency (ANR) as part of the “Investissements d’Avenir” program (ANR-11-LABX-0002-  
585 01, Lab of Excellence ARBRE). Antoine Billard’s PhD is funded by ADEME and Région  
586 Grand-Est. This work was also funded by the ExtraFor\_Est project coordinated by Francis  
587 Colin.

## 588 **Data availability:**

589 The datasets generated during and/or analysed during the current study are available  
590 from the corresponding author on reasonable request.

## 591 **Declaration on conflicts of interest:**

592 The authors declare that they have no conflict of interest.

## 593 **References**

- 594 Barnett, J., Gril, J., Saranpää, P., 2014. The biology of reaction wood introduction.
- 595 Barnett, J.R., Jeronimidis, G., 2003. Wood quality and its biological basis. CRC Press.
- 596 Billard, A., Bauer, R., Mothe, F., Jonard, M., Colin, F., Longuetaud, F., 2020. Im-  
597 proved aboveground biomass estimates by taking into account density variations be-  
598 tween tree components. *Annals of Forest Science* 77. doi:[https://doi.org/10.1007/  
599 s13595-020-00999-1](https://doi.org/10.1007/s13595-020-00999-1).
- 600 Bouriaud, O., Teodosiu, M., Kirdyanov, A., Wirth, C., 2015. Influence of wood density in  
601 tree-ring based annual productivity assessments and its errors in Norway spruce. *Biogeo-  
602 sciences* 12.

603 Cortini, F., Groot, A., Filipescu, C.N., 2013. Models of the longitudinal distribution of ring  
604 area as a function of tree and stand attributes for four major canadian conifers. *Annals of*  
605 *forest science* 70, 637–648.

606 Courbet, F., 1999. A three-segmented model for the vertical distribution of annual ring area:  
607 application to *Cedrus atlantica* Manetti. *Forest ecology and management* 119, 177–194.

608 Crawley, M.J., 2012. *The R book*. John Wiley & Sons.

609 Deng, X., Zhang, L., Lei, P., Xiang, W., Yan, W., 2014. Variations of wood basic density  
610 with tree age and social classes in the axial direction within *Pinus massoniana* stems in  
611 Southern China. *Annals of Forest Science* 71, 505–516. doi:[https://doi.org/10.1007/  
612 s13595-013-0356-y](https://doi.org/10.1007/s13595-013-0356-y).

613 Donaldson, L.A., Grace, J., Downes, G.M., 2004. Within-tree variation in anatomical prop-  
614 erties of compression wood in radiata pine. *IAWA journal* 25, 253–271.

615 Fabris, S., 2000. Influence of cambial ageing, initial spacing, stem taper and growth rate on  
616 the wood quality of three coastal conifers. Ph.D. thesis. University of British Columbia.

617 Filipescu, C.N., Lowell, E.C., Koppenaar, R., Mitchell, A.K., 2014. Modeling regional and  
618 climatic variation of wood density and ring width in intensively managed Douglas-fir.  
619 *Canadian journal of forest research* 44, 220–229.

620 Freyburger, Cand Longuetaud, F., Mothe, F., Constant, T., Leban, J.M., 2009. Measuring  
621 wood density by means of X-ray computer tomography. *Annals of Forest Science* 66, 804.

622 García-Gonzalo, E., Santos, A.J., Martínez-Torres, J., Pereira, H., Simões, R., García-Nieto,  
623 P.J., Anjos, O., 2016. Prediction of five softwood paper properties from its density using  
624 support vector machine regression techniques. *BioResources* 11, 1892–1904.

625 Gartner, B.L., North, E.M., Johnson, G.R., Singleton, R., 2002. Effects of live crown on  
626 vertical patterns of wood density and growth in Douglas-fir. *Canadian Journal of Forest*  
627 *Research* 32, 439–447. doi:<https://doi.org/10.1139/X01-218>.



- 628 González-Rodrigo, B., Esteban, L.G., de Palacios, P., García-Fernández, F., Guindeo, A.,  
629 2013. Variation throughout the tree stem in the physical-mechanical properties of the  
630 wood of *Abies alba* Mill. from the Spanish Pyrenees. *Madera y Bosques* 19, 87–107.
- 631 Gryc, V., Horáček, P., 2007. Variability in density of spruce (*Picea abies* [L.] Karst.) wood  
632 with the presence of reaction wood. *Journal of Forest Science* 53, 129–137.
- 633 Hamada, J., Pétrissans, A., Ruelle, J., Mothe, F., Colin, F., Pétrissans, M., Gérardin, P.,  
634 2018. Thermal stability of *Abies alba* wood according to its radial position and forest  
635 management. *European Journal of Wood and Wood Products* 76, 1669–1676.
- 636 Harris, J.M., 1977. Shrinkage and density of radiata pine compression wood in relation to  
637 its anatomy and mode of formation. *New Zealand Journal of Forestry Science* 7, 91–106.
- 638 Henin, J.M., Pollet, C., Jourez, B., Hébert, J., 2018. Impact of tree growth rate on the  
639 mechanical properties of Douglas fir lumber in Belgium. *Forests* 9, 342.
- 640 Henry, M., Bombelli, A., Trotta, C., Alessandrini, A., Birigazzi, L., Sola, G., Vieilledent, G.,  
641 Santenoise, P., Longuetaud, F., Valentini, R., Picard, N., Saint-André, L., 2013. Global-  
642 lomeTree: international platform for tree allometric equations to support volume, biomass  
643 and carbon assessment. *Forest Biogeosciences and Forestry* 6, 326–330.
- 644 Hernández, R.E., 2007. Swelling properties of hardwoods as affected by their extraneous  
645 substances, wood density, and interlocked grain. *Wood and Fiber Science* 39, 146–158.
- 646 Humar, M., Fabčić, B., Zupančič, M., Pohleven, F., Oven, P., 2008. Influence of xylem growth  
647 ring width and wood density on durability of oak heartwood. *International Biodeterioration  
648 & Biodegradation* 62, 368–371. doi:<https://doi.org/10.1016/j.ibiod.2008.03.010>.
- 649 Jacquin, P., Mothe, F., Longuetaud, F., Billard, A., Kerfriden, B., Leban, J.M., 2019. Car-  
650 Den: A software for fast measurement of wood density on increment cores by CT scanning.  
651 *Computers and Electronics in Agriculture* 156, 606–617.
- 652 Jozsa, L., Brix, H., 1989. The effects of fertilization and thinning on wood quality of a  
653 24-year-old Douglas-fir stand. *Canadian Journal of Forest Research* 19, 1137–1145.

- 654 Jozsa, L., Middleton, G., et al., 1994. A discussion of wood quality attributes and their  
655 practical implications. Forintek Canada Special Publication No.SP-34. .
- 656 Kerfriden, B., Bontemps, J.D., Leban, J.M., 2021. Variations in temperate forest stem  
657 biomass ratio along three environmental gradients are dominated by interspecific differences  
658 in wood density. *Plant Ecology* 222, 289–303.
- 659 Kimberley, M.O., Cown, D.J., McKinley, R.B., Moore, J.R., Dowling, L.J., 2015. Modelling  
660 variation in wood density within and among trees in stands of New Zealand-grown radiata  
661 pine. *New Zealand Journal of Forestry Science* 45, 1–13. doi:[https://doi.org/10.1186/  
662 s40490-015-0053-8](https://doi.org/10.1186/s40490-015-0053-8).
- 663 Kimberley, M.O., McKinley, R.B., Cown, D.J., Moore, J.R., 2017. Modelling the variation in  
664 wood density of New Zealand-grown Douglas-fir. *New Zealand Journal of Forestry Science*  
665 47, 15.
- 666 Lachenbruch, B., Moore, J.R., Evans, R., 2011. Radial variation in wood structure and func-  
667 tion in woody plants, and hypotheses for its occurrence, in: *Size-and age-related changes*  
668 *in tree structure and function*. Springer, pp. 121–164.
- 669 Larson, P.R., Kretschmann, D.E., Clark, A.I., Isebrands, J., 2001. Formation and properties  
670 of juvenile wood in southern pines: a synopsis. Gen. Tech. Rep. FPL-GTR-129. Madison,  
671 WI: US Department of Agriculture, Forest Service, Forest Products Laboratory. 42 p. 129.
- 672 Lee, P.W., Eom, Y.G., 1988. Anatomical comparison between compression wood and opposite  
673 wood in a branch of korean pine (*pinus koraiensis*). *IAWA journal* 9, 275–284.
- 674 Li, X., Evans, R., Gapare, W., Yang, X., Wu, H.X., 2014. Characterizing compression wood  
675 formed in radiata pine branches. *IAWA journal* 35, 385–394.
- 676 Liepiņš, J., Liepiņš, K., 2017. Mean basic density and its axial variation in Scots pine, Norway  
677 spruce and birch stems. *Research for Rural Development* 1. doi:[https://doi.org/10.  
678 22616/rrd.23.2017.003](https://doi.org/10.22616/rrd.23.2017.003).

- 679 Longuetaud, F., Mothe, F., Fournier, M., Dlouha, J., Santenoise, P., Deleuze, C., 2016.  
680 Within-stem maps of wood density and water content for characterization of species: a  
681 case study on three hardwood and two softwood species. *Annals of Forest Science* 73,  
682 601–614. doi:<https://doi.org/10.1007/s13595-016-0555-4>.
- 683 Longuetaud, F., Mothe, F., Santenoise, P., Diop, N., Dlouha, J., Fournier, M., Deleuze, C.,  
684 2017. Patterns of within-stem variations in wood specific gravity and water content for  
685 five temperate tree species. *Annals of Forest Science* 74. doi:<https://doi.org/10.1007/s13595-017-0657-7>.
- 687 Mitchell, M.D., Denne, M.P., 1997. Variation in density of *Picea sitchensis* in relation to  
688 within-tree trends in tracheid diameter and wall thickness. *Forestry: An International*  
689 *Journal of Forest Research* 70, 47–60.
- 690 Molteberg, D., Høibø, O., 2007. Modelling of wood density and fibre dimensions in mature  
691 Norway spruce. *Canadian Journal of Forest Research* 37, 1373–1389. doi:<https://doi.org/10.1139/X06-296>.
- 693 Niinemets, Ü., Valladares, F., 2006. Tolerance to shade, drought, and waterlogging of tem-  
694 perate Northern Hemisphere trees and shrubs. *Ecological monographs* 76, 521–547.
- 695 Niklas, K.J., Spatz, H.C., 2010. Worldwide correlations of mechanical properties and green  
696 wood density. *American Journal of Botany* 97, 1587–1594. doi:<https://doi.org/10.3732/ajb.1000150>.
- 698 Nogueira, E.M., Fearnside, P.M., Nelson, B.W., 2008. Normalization of wood density in  
699 biomass estimates of Amazon forests. *Forest Ecology and Management* 256, 990–996.  
700 doi:<https://doi.org/10.1016/j.foreco.2008.06.001>.
- 701 Pillow, M.Y., Luxford, R.F., 1937. Structure, occurrence, and properties of compression  
702 wood. Technical Report.
- 703 Pinheiro, J.C., Bates, D.M., 2000. *Mixed-effects models in S and S-PLUS*. Springer. ISBN0-  
704 387-98957-0 , 1–537.

705 Plourde, B.T., Boukili, V.K., Chazdon, R.L., 2015. Radial changes in wood specific gravity  
706 of tropical trees: inter-and intraspecific variation during secondary succession. *Functional*  
707 *Ecology* 29, 111–120.

708 Pressler, M., 1864. *Das gesetz der stamanpildung*. Amoldiscne Buchnanalung, Liepzig .

709 R Core Team, 2020. R: A language and environment for statistical computing. R Foundation  
710 for Statistical Computing. Vienna, Austria. URL: <https://www.R-project.org/>.

711 Repola, J., 2006. Models for vertical wood density of Scots pine, Norway spruce and birch  
712 stems, and their application to determine average wood density. *Silva Fennica* 40, 673–685.  
713 doi:<https://doi.org/10.14214/sf.322>.

714 Rueda, R., Williamson, G.B., 1992. Radial and vertical wood specific gravity in *Ochroma*  
715 *pyramidale* (Cav. ex Lam.) Urb.(Bombacaceae). *Biotropica* 24, 512–518. doi:<https://doi.org/10.2307/2389013>.

717 Saranpää, P., 2003. Wood density and growth. in Barnett and Jeronimidis (2003) , 87–117.

718 Seynave, I., Bailly, A., Balandier, P., Bontemps, J.D., Cailly, P., Cordonnier, T., Deleuze, C.,  
719 Dhôte, J.F., Ginisty, C., Lebourgeois, F., Merzeau, D., Paillassa, E., Perret, S., Richter,  
720 C., Meredieu, C., 2018. GIS Coop: networks of silvicultural trials for supporting forest  
721 management under changing environment. *Annals of Forest Science* 75, 48. doi:<https://doi.org/10.1007/s13595-018-0692-z>.

723 Sopushynskyy, I., Maksymchuk, R., Kopolovets, Y., Ayan, S., 2020. Intraspecific structural  
724 signs of curly silver fir (*abies alba* mill.) growing in the ukrainian carpathians. *Journal of*  
725 *Forest Science* 66, 299–308.

726 Sotelo Montes, C., Weber, J.C., Abasse, T., Silva, D.A., Mayer, S., Sanquetta, C.R., Muñoz,  
727 G.I., Garcia, R.A., 2017. Variation in fuelwood properties and correlations of fuelwood  
728 properties with wood density and growth in five tree and shrub species in niger. *Canadian*  
729 *Journal of Forest Research* 47, 817–827.

- 730 Taras, M.A., Wahlgren, H.E., 1963. A comparison of increment core sampling methods for  
731 estimating tree specific gravity. volume 7. US Department of Agriculture, Forest Service,  
732 Southeastern Forest Experiment.
- 733 Tarmian, A., Remond, R., Dashti, H., Perré, P., 2012. Moisture diffusion coefficient of  
734 reaction woods: compression wood of picea abies l. and tension wood of fagus sylvatica l.  
735 Wood science and technology 46, 405–417.
- 736 Tian, X., Cown, D.J., McConchie, D.L., 1995. Modelling of Pinus radiata wood properties.  
737 Part 2: Basic density. New Zealand Journal of Forestry Science 25, 214–230.
- 738 Todaro, L., Macchioni, N., 2011. Wood properties of young Douglas-fir in Southern Italy:  
739 results over a 12-year post-thinning period. European Journal of Forest Research 130,  
740 251–261.
- 741 Vieilledent, G., Fischer, F.J., Chave, J., Guibal, D., Langbour, P., Gérard, J., 2018. New  
742 formula and conversion factor to compute basic wood density of tree species using a global  
743 wood technology database. American Journal of Botany 105, 1653–1661.
- 744 Wahlgren, H.E., Fassnacht, D.L., 1959. Estimating tree specific gravity from a single incre-  
745 ment core. USDA Forest Service, Forest Products Laboratory report No. 2146 , 24 p.
- 746 Wassenberg, M., Chiu, H.S., Guo, W., Spiecker, H., 2015. Analysis of wood density profiles  
747 of tree stems: Incorporating vertical variations to optimize wood sampling strategies for  
748 density and biomass estimations. Trees 29, 551–561. doi:[https://doi.org/10.1007/  
749 s00468-014-1134-7](https://doi.org/10.1007/s00468-014-1134-7).
- 750 Westing, A.H., 1965. Formation and function of compression wood in gymnosperms. The  
751 Botanical Review 31, 381–480.
- 752 Wiemann, M.C., Williamson, G.B., 2014. Wood specific gravity variation with height and its  
753 implications for biomass estimation. USDA Forest Service, Forest Products Laboratory,  
754 Research Paper, FPL-RP-677, 2014; 12 p. 677, 1–12. doi:[https://doi.org/10.2737/  
755 FPL-RP-677](https://doi.org/10.2737/FPL-RP-677).

- 756 Williamson, G.B., Wiemann, M.C., 2010. Measuring wood specific gravity... correctly.  
757 American Journal of Botany 97, 519–524. doi:<https://doi.org/10.3732/ajb.0900243>.
- 758 Woodcock, D.W., Shier, A.D., 2002. Wood specific gravity and its radial variations:  
759 The many ways to make a tree. Trees 16, 437–443. doi:<https://doi.org/10.1007/s00468-002-0173-7>.  
760
- 761 Zanne, A.E., Lopez-Gonzalez, G., Coomes, D.A., Ilic, J., Jansen, S., Lewis, S.L., Miller,  
762 R.B., Swenson, N.G., Wiemann, M.C., Chave, J., 2009. Global wood density database  
763 doi:<https://doi.org/10.5061/dryad.234>.
- 764 Zobel, B.J., Van Buijtenen, J.P., 1989. Wood variation: Its causes and control. Springer  
765 Science & Business Media.